Solid State Communications 152 (2012) 1509–1512

Contents lists available at SciVerse ScienceDirect

Solid State Communications

journal homepage: www.elsevier.com/locate/ssc

Significant enhancement of electrical transport properties of thermoelectric $Ca_3Co_4O_{9+\delta}$ through Yb doping

Xueyan Song [a,*], Yun Chen [a], Song Chen [a], Ever Barbero [a], Evan L. Thomas [b], Paul Barnes [c]

[a] Dept Mechanical and Aerospace Engineering, West Virginia University, Evansdale Drive, Morgantown, WV 26506, USA
[b] University of Dayton Research Institute/Air Force Research Laboratory-WPAFB, Energy Technologies and Materials Division, 300 College Park, Dayton, OH 45469, USA
[c] Army Research Laboratory, 2800 Powder Mill Rd., Adelphi, MD 20783, USA

ARTICLE INFO

Article history:
Received 17 May 2012
Received in revised form
4 June 2012
Accepted 13 June 2012
communicated by Prof. P. Sheng
Available online 18 June 2012

Keywords:
Thermoelectric materials
Cobalt oxide
Substitution
Transmission electron microscopy

ABSTRACT

We report the significant enhancement of the power factor of $Ca_3Co_4O_{9+\delta}$ through Yb doping. The pellets were prepared by pressing under 0.5 GPa and 2 GPa. The highest power factor of 553 $\mu W\,m^{-1}\,K^{-2}$ due to the significant increase of electrical conductivity was obtained for $Ca_{2.9}Yb_{0.1}Co_4O_{9+\delta}$ pressed at 0.5 GPa. This is 2.3 times higher than that of $Ca_3Co_4O_{9+\delta}$ (246 $\mu W\,m^{-1}\,K^{-2}$). Nanostructure examinations show that the pellets pressed at 0.5 and 2 GPa have different nano-lamella structures. This work suggests that Yb is an effective doping element for enhancing the electrical transport properties of $Ca_3Co_4O_{9+\delta}$, and the optimum doping level is related to the nanostructure of the bulk pellets.

1. Introduction

Thermoelectric (TE) technology is recognized as a clean and promising energy conversion technology, which can convert waste heat from many energy production and consumption systems directly into electricity [1–4]. To achieve a high efficiency in a TE power generator, particularly for high temperature applications, identifying high performance TE materials is key. At high temperatures, many metal oxides offer good durability in air with low cost and minimized environmental impact. Misfit layered calcium cobaltite is one of the best p-type TE oxides and thus has been extensively studied [1–12]. The $Ca_3Co_4O_{9+\delta}$ single crystal shows very good TE behavior with an extrapolated *ZT* of 0.8 at 973 K [2], and is highly stable in air up to 1199 K [10]. A challenge for developing oxide TE material is to improve the conversion efficiency of polycrystal $Ca_3Co_4O_{9+\delta}$, which is currently low [11].

Enhancing the TE performance of $Ca_3Co_4O_{9+\delta}$ through doping transition metals and/or rare-earth metals at the Co site and Ca site could improve the TE performance of $Ca_3Co_4O_{9+\delta}$ [3–9]. It is stated that, by appropriate doping of the trivalent heavy Lanthanide elements for Ca^{2+} in the $Ca_3Co_4O_{9+\delta}$ system, an increase of the Seebeck coefficient could be achieved [7]. The substituting on the Ca site by rare earth metals may modify the Co oxidation state in two different ways: introducing trivalent elements could decrease the cobalt valence and also the carrier concentration, and increasing the $b1/b2$ ratio (distortion of lattice parameters) by doping smaller ionic radii rare-earth elements could increase the oxygen stoichiometry more quickly than the Co stoichiometry thus consequently increasing the Co valency [7,13,14].

In this study, we report the effect of Yb^{3+} doping on the Ca^{2+} site on the nanostructure and electrical properties of polycrystal $Ca_3Co_4O_{9+\delta}$. Particularly, the effect of Yb^{3+} doping associated with the pressure for cold pressing applied during fabrication of polycrystal $Ca_3Co_4O_{9+\delta}$ pellets is studied.

2. Experimental

The precursor powders with the nominal composition of $Ca_{3-x}Yb_xCo_4O_{9+\delta}$ ($x=0$, 0.1, 0.3 and 0.5) were prepared by a sol–gel chemical solution route. The gel was ashed at 773 K in a box furnace and the ashed product was calcined at 923 K in a tube furnace for 4 h with oxygen flow to form the precursor powders. The powders were then grounded and uniaxially pressed into pellets at either 0.5 GPa or 2 GPa. The pellets were sintered at 1193 K for 24 h in a box furnace to obtain the bulk samples. The absolute Seebeck coefficient *S* and electrical resistivity ρ were measured in the direction parallel to the pressed plane from 273 K up to 1073 K using a Linseis LSR-1100 in a He environment. X-ray diffraction (XRD) analysis was employed for phase identification. A JEOL JSM 7600F Scanning electron microscope (SEM),

* Corresponding author. Tel.: +1 304 293 3269; fax: +1 304 293 6689.
E-mail address: xueyan.song@mail.wvu.edu (X. Song).

0038-1098/$ - see front matter © 2012 Elsevier Ltd. All rights reserved.
http://dx.doi.org/10.1016/j.ssc.2012.06.014

and a JEM-2100 transmission electron microscope (TEM) equipped with energy dispersive X-ray spectroscopy (EDS) were used to examine the structure and chemistry from micron to atomic scale.

3. Results and discussion

Fig. 1(a) and (b) display the temperature dependence of the electrical transport properties for the samples pressed at 0.5 GPa and 2 GPa, respectively, with different doping levels. It can be seen that the S increases along with the increase of the Yb doping amount. One exception is the sample doped with 0.1 Yb and pressed at 2 GPa where a lower S is observed compared with the undoped sample. The S usually peaks at temperatures between 950 K and 1050 K. The highest S (193 $\mu V\,K^{-1}$) was obtained on the sample doped with 0.5 Yb and pressed at 0.5 GPa.

The resistivity ρ shows a more complex trend depending on the Yb doping amount and the pressure applied during pellet fabrication. Among the tested samples, the lowest ρ was obtained on the sample doped with 0.1 Yb and pressed at 0.5 GPa, yielding only about 50% of that from the baseline undoped sample throughout the entire temperature range of testing. To our knowledge, this is the lowest ρ reported in the polycrystal $Ca_3Co_4O_{9+\delta}$ system so far [15,16]. On the other hand, for the set of the samples pressed at 2 GPa, the most significant decrease in ρ is observed for doping at $x=0.3$ concentrations. Doping with 0.5 Yb results in the increase in ρ as the temperature increases. In the temperature range studied, the $Ca_{3-x}Yb_xCo_4O_{9+\delta}$ samples with $x<=0.3$ display a metallic-like character, while the samples with $x=0.5$ (both 0.5 and 2 GPa) exhibit semiconducting-like behavior.

For the sample pressed at 0.5 GPa with a doping level of 0.1, the optimum power factor (S^2/ρ)is 553 $\mu W m^{-1} K^{-2}$ at 904 K and is 2.3 times higher than the baseline sample (246 $\mu W\,m^{-1}\,K^{-2}$). For the samples pressed at 2 GPa, the optimum doping level is 0.3 with the power factor reaching 455 $\mu W\,m^{-1}\,K^{-2}$ at 879 K and is 1.68 times higher than the baseline sample (270 $\mu W\,m^{-1}\,K^{-2}$).

The apparent densities are roughly 3.2 $g\,cm^{-3}$ for the pellets cold pressed at 0.5 GPa and 3.88 $g\,cm^{-3}$ for the samples pressed at 2 GPa. Compared with the theoretical density [1] of 4.68 $g\,cm^{-3}$ for $Ca_3Co_4O_{9+\delta}$, the packing densities are ~68% and ~83% for the 0.5 GPa and 2 GPa samples, respectively. X-ray powder diffraction results (not shown) indicate that all the samples could be indexed as $Ca_3Co_4O_9$ phase (JCPDS card, No. 23–110). No obvious impurities could be found, even in the

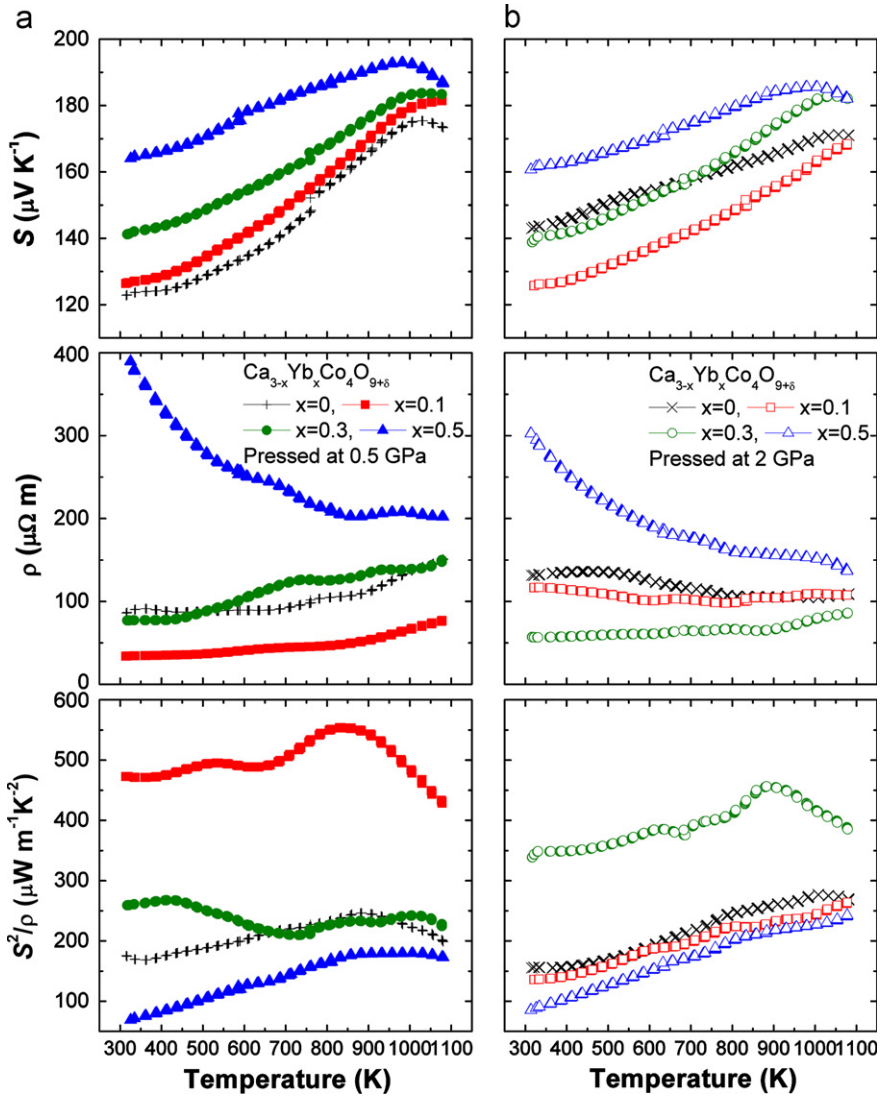

Fig. 1. Electrical transport properties of $Ca_{3-x}Yb_xCo_4O_{9+\delta}$, $x=0$, 0.1, 0.3 and 0.5. Columns a and b indicate the two sets of samples pressed at (a) 0.5 GPa and (b) 2 GPa, respectively.

sample with Yb doping of up to 0.5. The SEM images shown in Fig. 2 were taken from the fractured surface of the pellets. It is shown that the pellets pressed under 0.5 GPa and 2 GPa both form plate shaped grains of ~2 μm in the planar dimension and ~0.5 μm in thickness.

TEM examination shows that, each crystal grain in the SEM image actually consists of bundles of nano-lamellas. Fig. 3 and Fig. 4 present the representative nanostructure for the samples pressed at 0.5 GPa and at 2 GPa, respectively. All the examined samples exhibit the longer micron-sized dimension of the nano-lamella that are always perpendicular to the *c*-axis of the monoclinic $Ca_3Co_4O_9$ phase. The insert HRTEM images show that all nano-lamella in the same "bundle" have the *c*-axis parallel to the same direction. One of the distinct differences between the pellets pressed at 0.5 GPa and 2 GPa is the thickness of the nano-lamellas. For the pellets pressed at 0.5 GPa, the nano-lamellas are within the range of 5–40 nm. The thickness of the nano-lamella increased to about 50–250 nm in the samples pressed at 2 GPa. Such nano-lmella thickness difference indicates that the grain boundary (GB) density in pellets pressed at 0.5 GPa is significantly higher than those pressed at 2 GPa. No secondary phase was found within the nanolamella or at the grain boundaries, even with the doping level up to 0.5. The element Yb remains in the $Ca_3Co_4O_9$ lattice as the substitution dopant. For the pellets pressed under the same pelletizing conditions (0.5 GPa or 2 GPa), there is no obvious difference in terms of the grain alignment, the grain size, and nanostructure, could be observed using SEM or TEM, among the pellets with different Yb doping amount.

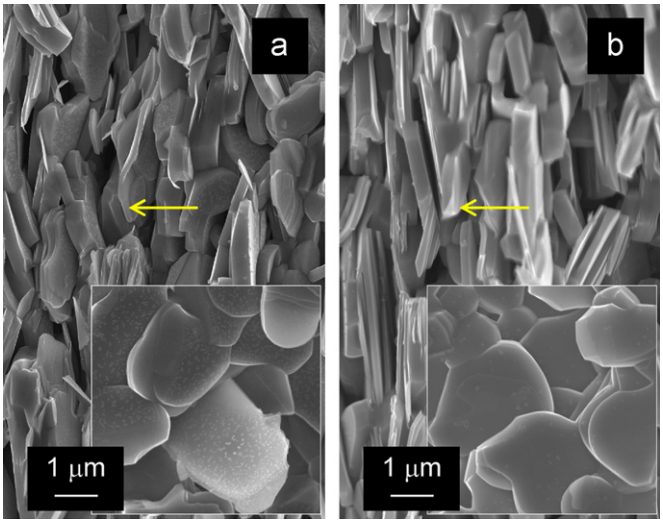

Fig. 2. SEM images showing the fractured cross sections of $Ca_{3-x}Yb_xCo_4O_{9+\delta}$, (a) $x=0.1$ and pressed at 0.5 GPa, and (b) $x=0.3$ and pressed at 2 GPa. Inserted images show morphologies of the corresponding pressed planes.

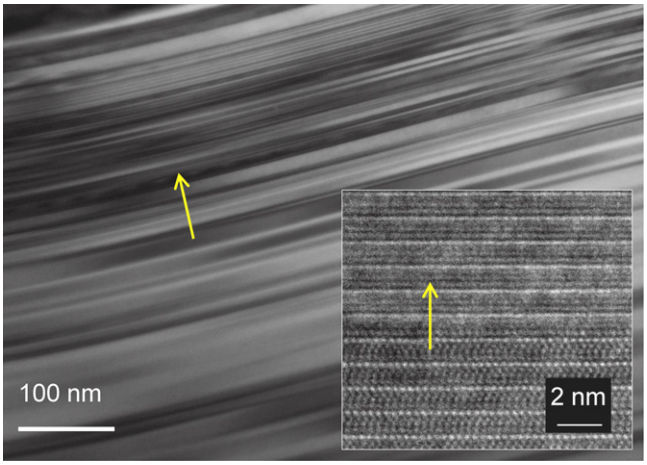

Fig. 3. TEM image for the sample doped with 0.1 Yb and pressed at 0.5 GPa. Insert: HRTEM image shows the microstructure near GB region. Yellow arrows point out the *c*-axis of the $Ca_{3-x}Yb_xCo_4O_{9+\delta}$.(For interpretation of the references to color in this figure legend, the reader is reffered to the web version of this article.)

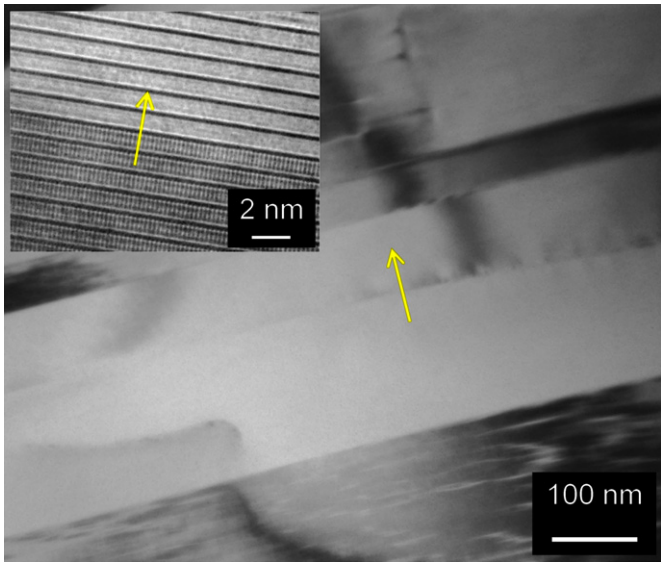

Fig. 4. TEM image for the sample doped with 0.3 Yb and pressed at 2 GPa. Insert: HRTEM image shows the microstructure near GB region.

The present study clearly shows that Yb doping affects both the carrier mobility (evidenced from the significant decrease of ρ) and carrier concentration (evidenced from the increase of S). The optimum doping level is also strongly related to the nanostructure that is controlled by the cold pressing. The optimum Yb doping amount for the samples pressed at 0.5 GPa and 2 GPa are different. Considering the relatively higher density of the samples pressed at 2 GPa, the sample doped with 0.1 Yb and pressed at 0.5 GPa surprisingly shows a remarkably lower ρ, implying a much higher electrical conductive property was achieved. Most importantly, the effect of doping is significantly impacted by the nanostructure, i.e., GB density and the nano-lamella thickness. TEM results show that a higher amount of GBs is present in the batch of pellets pressed at 0.5 GPa in which also the highest power factor is achieved. This implies that the GBs between nano-lamella, play an favorable role in the electrical transport. Also, the GB may interact with the dopants, and further affect the electrical transport properties. Since segregation of the dopant may occur at the GBs, the analysis of dopants concentration at the GBs is ongoing.

4. Summary

A substantial enhancement of electrical transport properties was reached through Yb doping of the Ca site in the $Ca_3Co_4O_{9+\delta}$ system. Yb doping affects both ρ and S, and the optimum doping level is strongly correlated with the nanostructure, controlled by the pressure of cold pressing. In the lower pressure formed samples, there are more GBs as evidenced by the thinner lamella structures. The higher doping in the higher pressured samples is necessary since there are fewer GBs and is a compensating factor to improve the performance (before overdoping occurs). A power

factor of 553 $\mu W\,m^{-1}\,K^{-2}$ was obtained for the sample doped with 0.1 Yb and pressed at 0.5 GPa. The present work clearly shows that doping of $Ca_3Co_4O_{9+\delta}$ with Yb is very promising, and the electrical properties can be tuned through both the doping and appropriate nanostructure control.

References

[1] A.C. Masset, C. Michel, A. Maignan, M. Hervieu, O. Toulemonde, F. Studer, B. Reveau, J. Hejtmanek, Phys. Rev. B 62 (2000) 166.
[2] M. Shikano, R. Funahashi, Appl. Phys. Lett. 82 (12) (2003) 1851.
[3] Y. Wang, Y. Sui, J.X. Wang, H.W. Su, X. Liu, J. Appl. Phys. 107 (2010) 033708.
[4] Y. Wang, Y. Sui, P. Ren, L. Wang, X.J. Wang, W.H. Su, H.J. Fan, Chem. Mater. 22 (3) (2010) 1155.
[5] C.J. Liu, L.C. Huang, J.S. Wang, Appl. Phys. Lett. 89 (2006) 204102.
[6] G.J. Xu, R. Funahashi, M. Shikano, I. Matsubara, Y.Q. Zhou, Appl. Phys. Lett. 80 (20) (2002) 3760.
[7] M. Prevel, O. Perez, J.G. Noudem, Solid State Sci. 9 (3-4) ((2007) 231.
[8] Y. Wang, Y. Sui, X.J. Wang, W.H. Su, Appl. Phys. Lett. 97 (5) (2010) 062114.
[9] N.V. Nong, N. Pryds, S. Linderoth, M. Ohtaki, Adv. Mater. 23 (21) (2011) 2484.
[10] E. Woermann, A. Muan, J. Inorg. Nucl. Chem. 32 (5) (1970) 1455.
[11] S. Katsuyama, Y. Takiguchi, M. Ito, J. Mater. Sci. 43 (10) (2008) 3553.
[12] N. Nong, M. Ohtaki, Solid State Commun. 139 (2006) 232.
[13] W. Koshibae, K. Tsutui, S. Maekawa, Phys. Rev. B 62 (2000) 6869.
[14] A. Maignan, D. Flahaut, S. Hebert, Eur. Phys. J. B39 (2004) 145.
[15] J.W. Fergus, J. Eur. Ceram. Soc. 32 (2012) 525.
[16] M. Ohtaki, J. Ceram. Soc. Jpn. 119 (11) (2011) 770.